

UC Berkeley

UC Berkeley Previously Published Works

Title

Indoor and outdoor particles in an air-conditioned building during and after the 2013 haze in Singapore

Permalink

<https://escholarship.org/uc/item/2t18g6d0>

Authors

Chen, Ailu
Cao, Qingliang
Zhou, Jin
[et al.](#)

Publication Date

2016-04-01

DOI

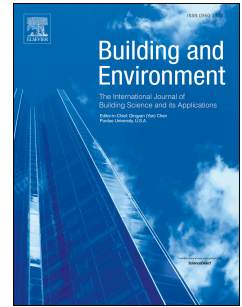
10.1016/j.buildenv.2016.01.002

Peer reviewed

Accepted Manuscript

Indoor and outdoor particles in an air-conditioned building during and after the 2013 haze in Singapore

Ailu Chen, Qingliang Cao, Jin Zhou, Bin Yang, Victor W.-C. Chang, William W. Nazaroff



PII: S0360-1323(16)30002-6

DOI: [10.1016/j.buildenv.2016.01.002](https://doi.org/10.1016/j.buildenv.2016.01.002)

Reference: BAE 4358

To appear in: *Building and Environment*

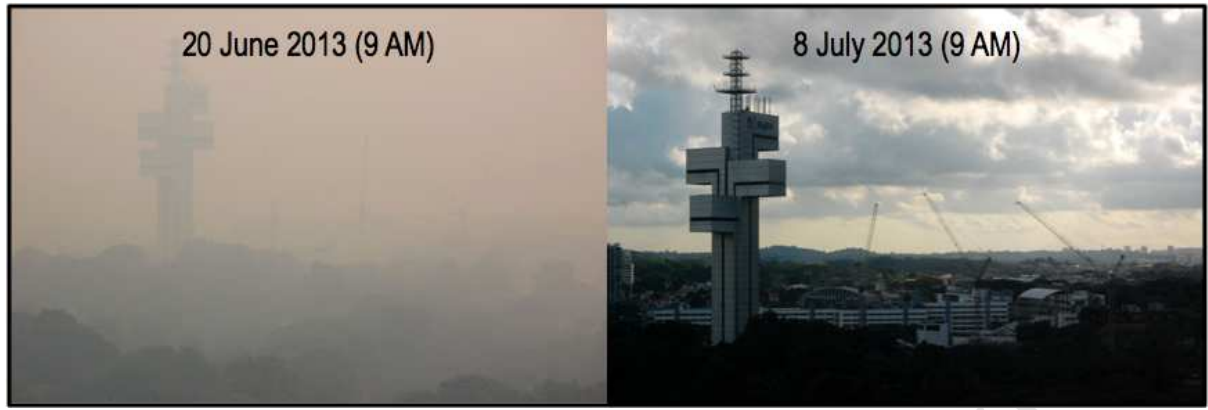
Received Date: 2 November 2015

Revised Date: 3 January 2016

Accepted Date: 4 January 2016

Please cite this article as: Chen A, Cao Q, Zhou J, Yang B, Chang VW-C, Nazaroff WW, Indoor and outdoor particles in an air-conditioned building during and after the 2013 haze in Singapore, *Building and Environment* (2016), doi: 10.1016/j.buildenv.2016.01.002.

This is a PDF file of an unedited manuscript that has been accepted for publication. As a service to our customers we are providing this early version of the manuscript. The manuscript will undergo copyediting, typesetting, and review of the resulting proof before it is published in its final form. Please note that during the production process errors may be discovered which could affect the content, and all legal disclaimers that apply to the journal pertain.



ACCEPTED MANUSCRIPT

1 Indoor and outdoor particles in an air-conditioned building during 2 and after the 2013 haze in Singapore

3 Ailu Chen^{1,2}, Qingliang Cao¹, Jin Zhou^{1,2}, Bin Yang³, Victor W.-C. Chang^{1,2*}, William W
4 Nazaroff^{2,4}

5 ¹School of Civil and Environmental Engineering, Nanyang Technological University, 50
6 Nanyang Avenue 639798, Singapore

7 ²SinBerBEST Program, Berkeley Education Alliance for Research in Singapore (BEARS), 1
8 CREATE Way, University Town 138602, Singapore

9 ³Department of Applied Physics and Electronics, Umeå University, Umeå 90187, Sweden

10 ⁴Department of Civil and Environmental Engineering, University of California, 760 Davis
11 Hall, Berkeley, California 94720, United States

12 *Corresponding Author: Tel: +65-6790-4773, Fax: +65-6792-1650, E-mail:

13 wcchang@ntu.edu.sg

14 Abstract

15 Particles released from biomass burning can contribute to severe air pollution. We monitored
16 indoor and outdoor particles in a mechanically ventilated and air-conditioned building during
17 and after the 2013 haze event in Singapore. Continuous monitoring of time-and size-resolved
18 particles in the diameter range 0.01-10 μm was conducted for two weeks in each sampling
19 campaign. During the haze event, the averaged size-resolved outdoor particle volume
20 concentrations ($dV/d(\log D_p)$) for diameters larger than 0.3 μm were considerably higher than
21 those during the post-haze days (9-185 $\mu\text{m}^3 \text{cm}^{-3}$ versus 1-35 $\mu\text{m}^3 \text{cm}^{-3}$). However, the
22 average number concentration of particles with diameters in the range 10-200 nm was
23 substantially lower on the hazy days than on the post-haze days (11,400 to 14,300 particles
24 cm^{-3} for hazy days, versus an average of 23,700 particles cm^{-3} on post-haze days). The
25 building mechanical ventilation system, equipped with MERV 7 filters, attenuated the
26 penetration and persistence of outdoor particles into the monitored building. Indoor particle
27 concentrations, in the diameter ranges 0.3-1.0 μm and 1.0-2.5 μm , closely tracked the

28 corresponding patterns of outdoor particle concentrations. For particles in the size range
29 0.01-1.0 μm , the size-resolved mean indoor/outdoor (I/O) ratios were in the range 0.12-0.65
30 with the highest mean I/O ratio at 0.3 μm (0.59 in AC on mode and 0.64 in AC off mode).
31 The air conditioning and mechanical ventilation system with MERV 7 filters provided low
32 single-pass removal efficiency (less than $\sim 30\%$) for particles with diameters of 0.01-1.0 μm .
33 During the haze, for particles larger than $\sim 0.2 \mu\text{m}$, lower I/O ratios and higher removal
34 efficiencies occurred with the air conditioning operating as compared to with mechanical
35 ventilation only. This observation suggests the possibility of particle loss to air conditioning
36 system surfaces, possibly enhanced by thermophoretic or diffusiphoretic effects.

37 **Keywords:** Indoor-outdoor relationship, Aerosol, Landscape fires, Pollutants, Particulate
38 matter

39 **1. Introduction**

40 Two types of large, uncontrolled combustion can contribute to regional-scale air pollution
41 episodes. Wildfires are common seasonal occurrences especially in semiarid regions such as
42 the western United States and Australia. The use of large-scale biomass burning to clear land
43 for agriculture is an important environmental issue in Southeast Asia. Such burning causes
44 air quality problems because of the heavy emissions of combustion byproducts followed by
45 atmospheric transport and dispersion plus photochemical transformation processes that create
46 regional pollution episodes. Prior studies have investigated certain characteristics of airborne
47 particulate matter associated with uncontrolled biomass burning, such as the organic and
48 elemental carbon (OC/EC) composition of air [1, 2], biomass burning signatures of individual

49 particles [3], trace elements in particulate matter [4, 5] and particle-bound polycyclic
50 aromatic hydrocarbons (PAHs) [5, 6].

51 Particles originating from biomass burning might have significant impacts on human health.
52 For example, such particles are demonstrated to be more toxic to lung macrophages than
53 other ambient particles [7]. Particles from wildfires can induce pro-inflammatory responses
54 [8] and contribute to oxidative stress [9]. A large wildfire in southern California was found
55 to result in a “significant increase in hospital emergency room visits for asthma, respiratory
56 problems, eye irritation, and smoke inhalation” [10]. Because of their potential contributions
57 to the degradation of public health, it is worthwhile to pursue a deeper understanding of
58 airborne particulate matter associated with uncontrolled biomass burning episodes.

59 Particle size is a key parameter, not only influencing dynamic behavior but also for assessing
60 human health risks [11]. A few studies have documented that biomass burning activities can
61 alter the airborne particle size distribution in the impacted area [12, 13]. Increases in particle
62 mass concentrations are observed in the accumulation mode (0.1-2.0 μm). Particles in this
63 size range contribute strongly to visibility impairment, a commonly observed adverse impact
64 of large-scale biomass burning. Increases are also reported for the coarse mode ($> 2.0 \mu\text{m}$).
65 However, decreases have been observed in the nucleation mode (diameter smaller than 0.1
66 μm). These findings highlight the importance of dynamic processes that influence the
67 evolution of the particle size distribution. For example, growth induced by the condensation
68 of semivolatile vapors would tend to shift nucleation mode particles toward the accumulation

69 mode. It is important to better understand the size distributions of airborne particles
70 associated with biomass burning events.

71 The penetration and persistence of particles from outdoor to indoor air is important with
72 regard to health because people spend a large fraction of their time indoors [14]. When
73 outdoor pollution levels are high, as during biomass burning episodes, people may be advised
74 to curtail activities and remain indoors as a “shelter-in-place” strategy. For an office
75 building, the major pathway connecting the indoor environment to outdoor air is the heating,
76 ventilating and air-conditioning (HVAC) system [15]. For tropical climates such as in
77 Singapore, heating is seldom or never needed, and so the analogous term, which we shall use
78 in this paper, is the air-conditioning and mechanical ventilation (ACMV) system.

79 Several studies have reported that submicron particle number concentrations in office
80 buildings closely follow the corresponding outdoor concentrations in the absence of a strong
81 indoor source [16, 17, 18]. Among the factors that can affect the particle indoor/outdoor
82 ratios (I/O) are particle size [19], air-exchange rate (AER) [19], and filter efficiency [16].
83 Indoor concentrations of particles originating outdoors can be reduced by improving filter
84 efficiency [20]. Shi et al. [21] have reported laboratory tests that document the size-
85 dependent particle removal efficiency of filters commonly used in ventilation systems.

86 However, indoor-outdoor relationships have not been extensively reported for office
87 buildings in relation to air pollution episodes caused by uncontrolled biomass burning. It is
88 worthwhile to better understand the performance of normally used filters in office buildings

89 for removing particles of outdoor origin, especially when the outdoor levels are episodically
90 elevated, as during the 2013 haze in Singapore.

91 During the Southeast Asia haze episode of June 2013, the outdoor $PM_{2.5}$ concentrations rose
92 to $250 \mu\text{g m}^{-3}$ on the most polluted days. This order-of-magnitude elevation above the
93 normal ambient $PM_{2.5}$ concentration of $15\text{-}25 \mu\text{g m}^{-3}$ provided an opportunity to investigate
94 the relationship between indoor and outdoor particle levels in a mechanically ventilated and
95 air-conditioned building when the outdoor particle level was unusually high. The current
96 study presents monitoring results and their interpretation considering size- and time-resolved
97 indoor and outdoor particle concentrations both during the 2013 haze and on low-pollution
98 days after the haze episode. The study aims to provide information and contribute new
99 knowledge regarding four important features at the intersection of regional air pollution
100 episodes, building environmental systems, and human exposure: 1) size-resolved outdoor
101 particle volume and number concentrations measured in Singapore with and without episodic
102 haze; 2) size-resolved indoor and outdoor particle relationships in a typical office building; 3)
103 influence of ACMV operation modes on these relationships (i.e., with and without operating
104 the air-conditioning cooling coil); and 4) performance of a typical ACMV system on
105 reducing the penetration and persistence of outdoor particles indoors.

106 2. Material and Methods

107 2.1. Monitoring sites

108 Outdoor and indoor monitoring was undertaken on the campus of Nanyang Technological
109 University (NTU). The NTU campus, located in western Singapore, is bordered by forested
110 land to the north and west, by industrial areas to the south, and by residential areas to the east.

111 On hazy days, the adjacent areas are not likely to have contributed substantially to the
112 outdoor particle concentrations, as evidenced by the small variation in $PM_{2.5}$ concentrations
113 across the five government-operated monitoring stations that span the city [22]. The
114 sampling sites were on the western side of the campus, situated about 200 m from the forest.
115 Vehicular traffic on the campus is small, consisting mainly of light-duty passenger cars for
116 commuters. There are no other noteworthy particle sources on campus.

117 The present study reports results from two monitoring campaigns, with conditions that we
118 will refer to as “hazy” and “clear sky,” respectively. The hazy campaign spanned 14-29 June
119 2013 and the clear sky campaign took place 13-26 August 2013. Monitoring sites were the
120 same for both campaigns. The outdoor monitoring station was sited on the balcony of a
121 lecture theatre, with the air inlet positioned 12 m above the ground. The indoor station was
122 20 m away from the outdoor monitoring station and about 1.2 m above the floor. The fresh
123 air intake of the ACMV system was situated at a height of 21 m above the ground and at 20
124 m horizontal distance from the outdoor monitoring station. Given the strong regional impact
125 of the air pollution episode and the small contribution of local sources, we believe that the
126 outdoor monitoring results reflect accurately the conditions prevailing in the ventilation air

127 supplied to the indoor site. The room where the indoor station was placed had a hard-surface
128 floor of area 19 m^2 and was part of a staff office. The office had an area of 300 m^2 and had
129 been unoccupied for more than one year. Polyvinyl chloride flooring covered five-sixths of
130 the office's floor surfaces and the remaining floor area was carpeted. The office also
131 contained basic furniture such as tables, cabinets, and chairs. There were no obvious indoor
132 particle sources. The room had casement windows and curtains; windows and doors were
133 closed throughout both monitoring campaigns.

134 The air-handling unit (AHU) that served the office had an independent ventilation system
135 (Figure 1), so the office was isolated from other rooms in the same building. When the
136 mechanical ventilation was operating, make-up air accounted for $\sim 10\%$ of the volume flow
137 rate of supply air. The make-up air mixed with the recirculated air first and then the air
138 mixture passed through the filter and coil as shown in Figure 1. When the MV system was
139 on, the office was slightly pressurized by the supplied air; such pressurization would have
140 prevented outdoor air from substantially infiltrating into the office, making flow through the
141 ACMV system the dominant pathway of fresh air supply and outdoor particle penetration.
142 The filters in the AHU had a grade of MERV 7, which means its nominal removal efficiency
143 is 25-35% for particles with diameters of $0.3\text{-}10.0 \mu\text{m}$. In addition, its minimum removal
144 efficiencies for particles with diameters of $0.3\text{-}1.0 \mu\text{m}$, $1.0\text{-}3.0 \mu\text{m}$ and $3.0\text{-}10.0 \mu\text{m}$ are 17%,
145 46% and 50%, respectively [23].

146 When air conditioning was employed, chilled water circulating through the coil had a
147 temperature of 7 °C. In normal practice at NTU, filters are replaced and cooling coils are
148 cleaned concurrently at intervals of three months. From June to August 2013, the filters were
149 not replaced and the cooling coils were not cleaned. When the mechanical ventilation was on,
150 the air exchange rate of the office was 3.8 h⁻¹, whereas when the system was off, the average
151 air exchange rate (owing to leakage) was 0.5 h⁻¹.

152 The ACMV system was operated in three different modes during the two monitoring
153 campaigns. During weekdays of both the hazy and the clear-sky periods, the ACMV system
154 was on (Mode 1: air conditioning and mechanical ventilation on) from 7:30 to 18:30.
155 Overnight during the haze period, i.e. 18:30 to 7:30 on the next day, the AC was off but the
156 MV system continued to operate (Mode 2: air conditioning off, mechanical ventilation on).
157 During the weekday overnight intervals of the clear-sky period, the ACMV system was off
158 (Mode 3: air conditioning and mechanical ventilation off). For weekends (both daytime and
159 overnight), Mode 2 was applied during the haze period and Mode 3 was applied for the clear-
160 sky days.

161 2.2. Instruments

162 During both campaigns, size- and time-resolved concentrations of both indoor and outdoor
163 particles with diameters in the range 0.01 µm to 10 µm were concurrently monitored for
164 multiple days. Particles with diameters of 0.01 µm to 0.2 µm were measured with TSI
165 Nanoscan SMPS Nanoparticle Sizers (Model 3910, TSI Inc., Shoreview, USA). The SMPS

166 uses isopropyl alcohol (purity $\geq 99.7\%$, Sigma-Aldrich) as the reagent and can measure
167 particle number concentrations in the range 100-1,000,000 cm^{-3} . For larger particles, 0.3-10
168 μm in diameter, TSI optical particle sizers (OPS, Model 3330) were employed. These can
169 measure particle concentrations up to 3,000 cm^{-3} and optically resolve particles into 16 size
170 channels. Temperature and relative humidity were measured using TSI VelociCalc Air
171 Velocity meters (model 9545-A). Monitoring was conducted continuously every day and
172 measurement results were recorded at intervals of 1 min. However, with high water vapor
173 content in Singapore's air, we found that the SMPSs only functioned properly (i.e. without
174 reporting error) during some portions of each day. Consequently, we have relatively small
175 datasets from the SMPSs in the current study.

176 An InfraRan Specific Vapor Analyzer (Wilkes Enterprise Inc., East Norwalk, USA) was used
177 to measure the air exchange rates of the indoor environment based on the tracer gas decay
178 method, using sulfur hexafluoride as the tracer.

179 *2.3. Outdoor weather conditions*

180 In accordance with expectations for Singapore's tropical climate, the outdoor weather
181 conditions were similar during each sampling campaign. Table S1 presents a summary of
182 selected outdoor atmospheric parameters and $\text{PM}_{2.5}$ mass concentrations for the two
183 campaigns. The $\text{PM}_{2.5}$ mass concentration presented in Table S1 of each day was calculated
184 based on outdoor sized-resolved particle number concentrations monitored by outdoor OPS
185 and SMPS with assumed particle density of 1.0 g cm^{-3} [22]. During the hazy period,

186 temperatures were between 25 and 35 °C and the relative humidity was 40-90%. The
187 average daily wind speed was mainly in the range 5-8 km h⁻¹ (except for 19-20 June) and
188 from the southwest. Though it was during the monsoon season, there were only four
189 precipitation events (June 16, 24, 25 and 26). During the clear-sky campaign, air
190 temperatures were mainly between 27 and 32 °C and relative humidity was mainly between
191 50 and 90%. Mean wind speeds were mainly 4-8 km h⁻¹ and were primarily from the south.
192 There were six precipitation episodes during the clear-sky monitoring campaign. Given the
193 similar weather conditions, the influence of meteorological conditions on outdoor particles is
194 expected to be comparable for the two campaigns.

195 *2.4. Data analysis and quality assurance*

196 A clear difference is seen between the overall outdoor PM_{2.5} concentrations of these two
197 campaigns (Table S1). According to data reported by Singapore's National Environmental
198 Agency (NEA), during the 2013 haze episode, the daily averaged outdoor PM_{2.5}
199 concentrations ranged from 38 to 268 µg m⁻³ and the average PM_{2.5} concentration was 96 µg
200 m⁻³. Utilizing NEA data, and based on the daily-average outdoor PM_{2.5} concentrations, we
201 classified the hazy days into three categories: heavy haze (PM_{2.5} > 150 µg m⁻³), moderate
202 haze (60-150 µg m⁻³) and light haze (35-60 µg m⁻³). During the clear-sky periods, the daily
203 averaged outdoor PM_{2.5} concentrations normally ranged from 10 to 30 µg m⁻³ and the average
204 PM_{2.5} concentration was approximately 20 µg m⁻³.

205 Measured particle, temperature and RH results were first processed to exclude errors owing
206 to instrument malfunction. Indoor and outdoor data were then paired as linked time series.
207 For particles in the diameter range 0.01-10 μm , count concentrations were converted to
208 volume concentrations based on the method reported in Zhou et al [22]. All data were
209 arranged day-by-day and days that had complete data without evidence of error (i.e. owing to
210 instrument malfunction) were chosen to compute outdoor size-resolved particle volume
211 concentrations ($dV/d\log D_p$) and number concentrations ($dN/d\log D_p$). Size-resolved outdoor
212 particle data for 19-22 June were averaged to represent the heavy haze days; data for 16-18
213 and 23 June were averaged to represent moderate haze conditions, data on 24-25 and 27-29
214 June were used to represent light-haze days, and measurements from 16-17 and 21-23 August
215 were applied to represent the clear-sky conditions. In all, seventeen days were selected for
216 further analysis, considering data availability as the major criterion. Days that had
217 continuously valid data for less than three hours were excluded to limit errors in determining
218 I/O ratios owing to lag time. In preliminary data processing, we only accepted data for which
219 there was no error reported by either particle-monitoring instrument or otherwise recorded in
220 our logbook.

221 Data records for the time period 10:00 to 18:00 on days with valid data were chosen for
222 calculating I/O ratios for Mode 1. Data records from 20:00 to 6:00 of their next day were
223 chosen for analysis for Mode 2 conditions. Data recorded close to the transition periods of
224 the ACMV system (i.e., 6:00-10:00 each weekday morning and 18:00-20:00 each weekday
225 evening) were excluded to avoid potential biases caused by time-varying indoor

226 temperatures. One-way ANOVA tests were performed to compare size-resolved I/O ratios
227 under different ACMV operation modes. We applied a probability of 0.05 as the threshold in
228 testing for statistical significance (SPSS 22, IBM Inc., USA).

229 We conducted side-by-side tests for both the SMPSs and OPSs during light-haze and clear-
230 sky periods with outdoor $PM_{2.5}$ concentrations between $20 \mu\text{g m}^{-3}$ and $60 \mu\text{g m}^{-3}$. Adjustment
231 factors based on these comparisons were applied to minimize the differences between
232 individual instruments throughout the whole monitoring period. The side-by-side tests were
233 carried out in the room where the indoor station was placed. The test duration for the SMPSs
234 was 22.5 h and that for the OPSs was 21 h. In the tests, the monitors recorded data at 1-min
235 intervals, which was consistent with the indoor and outdoor monitoring experiments. We
236 calculated the adjustment factor for each channel using the average of readings in that
237 channel from the paired monitors as a reference value. In each channel, the reference values
238 were averaged over the whole test period and the average was divided by average of readings
239 from each monitor. The calculated adjustment factors are listed in Table S2. The paired
240 monitors were reasonably consistent with each other for both SMPSs and OPSs with most
241 differences smaller than 15%.

242 *2.5. Estimates of particle removal efficiencies of the ACMV system*

243 We estimated size-resolved single-pass particle removal efficiencies of the ACMV system,
244 which are believed to be mainly attributable to the MERV 7 filters. Various ACMV
245 components, including filters, coils, and ducting, may contribute to particle removal when the

246 system was operating; however, filters are believed to contribute the most to removal as other
 247 components should play limited roles, especially for fine particles [24, 25]. The filters
 248 remove the majority of coarse particles as they are the first layer of defense in the ACMV
 249 system (as shown in Figure 1) and they have much higher removal efficiency for coarse
 250 particles than for fine and ultrafine particles.

251 Equation 1, based on material balance, describes the time dependent indoor particle number
 252 concentration:

$$\frac{dN_{i,in}}{dt} = \lambda N_{i,out}(1 - \eta_i) - \lambda_r N_{i,in} \eta_i - \beta_i N_{i,in} - \lambda N_{i,in} \quad (1)$$

253 Here, $N_{i,in}$ is the indoor number concentration of particles in the i^{th} size bin (particles cm^{-3}); t
 254 is time (h); $N_{i,out}$ is the outdoor number concentration of particles in the i^{th} size bin (particles
 255 cm^{-3}); λ is the air-exchange rate (h^{-1}); η_i is single-pass removal efficiency of the ACMV
 256 system for particles in size bin i (unitless); λ_r is the recirculation rate of the indoor air in the
 257 ACMV system (h^{-1}); and β_i is the indoor deposition rate of particles in the i^{th} size bin (h^{-1}). In
 258 developing Equation 1, we assumed balanced volumetric flows (appropriate for near-
 259 isothermal conditions), no particle resuspension or generation indoors, no coagulation of
 260 particles, and no phase-change processes. We also assumed that during monitoring, when the
 261 mechanical ventilation was on, there was no particle infiltration from outdoors to indoors that
 262 would bypass the filter. In addition, we assumed that the air-exchange rate of the indoor
 263 environment was constant. We treated the filter efficiencies for particles of specific sizes to

264 be identical for makeup and recirculated air, since there are no separate prefilters in the
 265 system.

266 To solve Equation 1, we apply time averaging, neglecting any change of particle number
 267 concentration in the indoor environment and assuming that $N_{i,in}$ and $N_{i,out}$ are not correlated in
 268 time with λ , η_i , λ_r or β_i . The result is Equation 2:

$$\frac{\overline{N_{i,in}}}{\overline{N_{i,out}}} = \frac{\lambda(1-\eta_i)}{\lambda_r\eta_i + \beta_i + \lambda} \quad (2)$$

269 Here, $\overline{N_{i,in}}$ is the indoor time-averaged number concentration of particles in the i^{th} size bin
 270 (particles cm^{-3}) and $\overline{N_{i,out}}$ is the corresponding outdoor value (particles cm^{-3}). Considering
 271 $\overline{N_{i,in}} / \overline{N_{i,out}} = (I/O)_i$, we transformed Equation 2 to Equation 3 for calculating removal
 272 efficiency of the ACMV system for particles in each size bin:

$$\eta_i = \frac{\lambda - (\beta_i + \lambda)(I/O)_i}{\lambda + \lambda_r(I/O)_i} \quad (3)$$

273 Here, $(I/O)_i$ is time-averaged ratio of indoor to outdoor particle concentrations in the i^{th} size
 274 bin (unitless). Before undertaking the calculations, we first estimated the size-resolved
 275 indoor particle deposition rates (β_i). In this study, the β_i values are based on the deposition
 276 model developed by [Riley et al. \[26\]](#). Table S3 presents the calculated β_i value for each
 277 effective particle size. In the indoor environment, as shown in Figure 1, the air exchange rate
 278 was 3.8 h^{-1} and the recirculation rate was 34.2 h^{-1} . Size-resolved particle removal efficiencies
 279 of the ACMV system when it was operated in both Mode 1 (both AC on and MV on) and

280 Mode 2 (AC off and MV on) were computed based on the corresponding measured particle
281 I/O ratios, utilizing Equation 3.

282 3. Results and Discussion

283 3.1. Summary of indoor and outdoor particle number concentrations

284 Table S4 summarizes the time-weighted and size-resolved indoor and outdoor particle
285 number concentrations during and after the 2013 haze. For all haze levels, particles smaller
286 than 0.37 μm account for most particles by number. In each size range, the indoor
287 concentrations were always lower than the corresponding outdoor concentrations.

288 3.2. Size-resolved outdoor particle concentrations

289 Figure 2 illustrates time-averaged volume-weighted size distributions ($dV/d\log D_p$) measured
290 outdoors for particles with diameters 0.01-10 μm for the four haze conditions. Overall,
291 particle volume concentrations for the heavy haze days are approximately seven times higher
292 than on clear-sky days, with ratios ranging from 4 to 60 across particle sizes. Compared with
293 the clear-sky days, the total volume concentration is two times higher for light haze and five
294 times higher for moderate haze. It is noteworthy that submicron particles account for
295 approximately half (45-54%) of the total volume distribution for hazy days, whereas the
296 percentage was smaller (35%) for clear-sky conditions. There is an evident shift in the peak
297 of the submicron size distribution as the haze level increases. The peak diameter was 0.18
298 μm for clear-sky conditions and progressively increased to approximately 0.42 μm for the
299 moderate and heavy haze days. This observation suggests the occurrence of substantial

300 secondary growth of particles probably owing to a combination of condensation and
301 coagulation during the haze episode.

302 Figure 3 illustrates the time-averaged and size-resolved particle number distribution ($dN/d\log$
303 D_p) for particles with diameters of 0.01-10 μm , again sorted according to haze level. The
304 striking feature of this figure is the prominence of a count-weighted peak, centered at a
305 diameter of about 0.07 μm diameter, for clear-sky conditions. For hazy conditions, the peak
306 shifts to a larger particle size of about 0.2 μm diameter, for which light scattering would be
307 much more efficient.

308 Total number concentrations of ultrafine particles (0.01-0.2 μm) for hazy days were less than
309 measured for clear-sky conditions. Specifically, levels were $13,100 \pm 6,500$, $11,400 \pm 4,800$,
310 and $14,300 \pm 10,800$ particles cm^{-3} for heavy, moderate and light haze days, respectively,
311 versus $23,700 \pm 9,200$ particles cm^{-3} for clear-sky conditions. Qualitatively similar
312 observations have been reported by Betha et al. [27] and Mielonen et al. [28].

313 A plausible factor contributing to the shift in sizes is the different sources of ultrafine
314 particles and the associated growth processes. On hazy days, the primary source of
315 submicron particles over Singapore would be the agricultural fires in Sumatra, approximately
316 300 km to the west (as shown in Figure S1). It would take a day or two for pollutants emitted
317 from this locale to travel to Singapore. The time scale would enable the ultrafine particles to
318 grow to sizes larger than 0.10 μm in diameter [29]. Figure 3 shows that the count-weighted
319 size distribution has a peak at approximately 0.17 μm for both the heavy and moderate haze

320 days, whereas the peak occurs at $0.07\ \mu\text{m}$ on the clear-sky days. For clear-sky conditions,
321 probable sources of ultrafine particles measured in Singapore would be local emissions,
322 including industrial and vehicular activities [30]. The proximity of these sources to the
323 monitoring station offers much less time for ultrafine particle to grow through
324 photochemically driven condensation.

325 Additional evidence about the importance of time for condensational growth of haze particles
326 can be found in comparing the 2013 haze episode here to a 2009 haze event triggered by local
327 biomass burning in Singapore [30]. During the 2009 haze, the mean hourly total particle
328 number concentration was $37,800\ \text{particles cm}^{-3}$ ($5.6\text{-}560\ \text{nm}$), which was $3\times$ that in the
329 current study. During the 2009 haze, there was little time for newly generated ultrafine
330 particles to grow to submicron particles given the close proximity between the monitoring
331 and emissions sites. Differences in the peak diameters of the count-weighted size distribution
332 ($0.17\ \mu\text{m}$ during the 2013 haze *versus* $0.06\ \mu\text{m}$ during the 2009 episode) highlight the
333 importance of reaction time as a factor influencing particle size distributions.

334 The findings shown in Figures 2 and 3 indicate that particles larger than $0.1\ \mu\text{m}$ contributed
335 the most to the outdoor particle pollution during the 2013 haze episode. The findings
336 improve our understanding of the size distributions of particles originating from agricultural
337 biomass burning upwind of Singapore. Because of the frequent recurrence of transboundary
338 haze in Singapore, knowledge about particle size-distributions is useful for developing
339 technology and policy to mitigate the adverse effects of haze particles. In Section 3.3, we

340 evaluate indoor-outdoor relationships for particles in a mechanically ventilated building.

341 Since the ultrafine particle concentrations were observed not to increase during the haze, we

342 focus on particles with diameters of 0.3-10 μm and consider whether there are systematic

343 differences among the four different outdoor pollution conditions.

344 *3.3. Time-resolved outdoor and indoor particle concentrations*

345 Figure 4 shows time-resolved indoor and outdoor particle volume concentrations ($\mu\text{m}^3 \text{cm}^{-3}$)

346 in three size bins (0.3-1.0 μm , 1.0-2.5 μm and 5.0-10.0 μm) for one typical day each for the

347 heavy, moderate, and light haze conditions. In Figure 4, the ACMV was operating in Mode 1

348 (AC on + MV on) for 07:30-18:30 and in Mode 2 (AC off + MV on) for other times.

349 Figure 4 frames a, b, and c show that indoor particle concentrations in the size range 0.3-1.0

350 μm were always lower than the corresponding outdoor concentrations. Furthermore,

351 concentrations of these smaller sized particles tracked the corresponding outdoor

352 concentrations closely throughout the day. Temporal patterns of indoor concentrations were

353 attenuated and delayed when compared with the corresponding outdoor concentrations. The

354 indoor concentration was approximately half of the outdoor concentration. This attenuation

355 is mainly attributable to the ACMV system's filtration effects on outdoor particles in the

356 process of transporting air from outdoors to indoors and recirculating it; otherwise, the indoor

357 environment is well isolated from the outdoors by the building envelope. The data also

358 reveal a time lag of approximately 15 min between sudden changes in outdoor concentrations

359 and corresponding changes indoors. That lag is consistent expectations: it is approximately

360 the reciprocal of the measured air-exchange rate of 3.8 h^{-1} . For the three haze conditions,
361 indoor average volume concentrations for particles sized $0.3\text{-}1.0 \mu\text{m}$ were $43.6 \mu\text{m}^3 \text{ cm}^{-3}$,
362 $20.5 \mu\text{m}^3 \text{ cm}^{-3}$, and $5.5 \mu\text{m}^3 \text{ cm}^{-3}$, respectively; each of these values is higher than that for the
363 clear-sky conditions ($4.8 \mu\text{m}^3 \text{ cm}^{-3}$).

364 For particles with diameters in the range $1.0\text{-}2.5 \mu\text{m}$, indoor concentrations were much lower
365 than corresponding outdoor concentrations (Figure 4 frames d, e, and f). Impaction and
366 interception control particle filtration efficiency in this size range and are much more
367 efficient for these particles than for those in the $0.3\text{-}1 \mu\text{m}$ diameter range, for which the
368 ACMV system exhibited a weaker attenuation effect [31]. For the $1.0\text{-}2.5 \mu\text{m}$ diameter range,
369 indoor peak concentrations are approximately 20% of the corresponding outdoor peak
370 concentrations. Despite attenuation, indoor concentrations were still notably higher when the
371 outdoor concentrations were elevated during the haze. For heavy, moderate and light haze
372 days, the indoor mean volume concentrations in this size bin were 8.1, 7.6 and 1.1 times the
373 clear-sky values, respectively.

374 For particles in the diameter range $2.5\text{-}10.0 \mu\text{m}$, there is no evident temporal covariation
375 between indoor and outdoor concentrations (Figure 4 frames g, h, and i). The indoor volume
376 concentrations of particles in the diameter range $2.5\text{-}10.0 \mu\text{m}$ were consistently lower than 5
377 $\mu\text{m}^3 \text{ cm}^{-3}$ and were comparable across the different haze intensities, even though the outdoor
378 concentrations were markedly different for these days. These findings indicate that the
379 ACMV system in this building effectively protects occupants against outdoor particles larger

380 than 2.5 μm . The effectiveness of the ACMV system in limiting penetration and persistence
381 of these coarse particles from outdoors results from the high proportion of recirculation flow
382 (90%). Even though the single-pass efficiency of the MERV 7 filters is only moderate, the
383 multiple passes of indoor air through the filters yields a high overall effectiveness in reducing
384 airborne coarse particle concentrations.

385 In Section 3.2, we reported that particles larger than 0.1 μm dominated the particle volume or
386 mass concentrations during the haze. Here, we have shown that the ACMV system was
387 effective at removing particles larger than 2.5 μm under normal operation. Combining this
388 information, we could state that, in the absence of important indoor particle sources,
389 occupants of a building with a conventional ACMV system during the haze episode would
390 mainly be exposed to particles in the diameter range 0.1-2.5 μm . Recognizing the importance
391 of adverse human health effects associated with exposure to fine particles, it would be of
392 scientific and public health value to develop improved strategies to mitigate indoor fine
393 particle pollution from outdoor sources in this size range, especially during occasions of
394 extreme outdoor pollution such as the Singapore 2013 haze. Such information might assist
395 government agencies in setting policies to protect building occupants from excessive particle
396 exposure during haze episodes.

397 *3.4. Particle I/O ratios*

398 Figure 5 shows the time averaged and size-resolved I/O ratios of particles with diameters of
399 0.01-6.0 μm for two ACMV operation modes (Mode 1: both AC and MV on; Mode 2: AC off

400 and MV on). Table 1 reports the time, date and haze levels of the datasets for the I/O ratios
401 calculation. The small number of entries in Table 1 occurs because we only used datasets
402 when the both indoor and outdoor SMPSs were functioning properly. In both modes, the
403 ACMV system is the major pathway by which outdoor particles migrate indoors.

404 The I/O ratios for all particle sizes are smaller than one, as expected given the absence of any
405 notable indoor particle source. For particles in the size range 0.01-0.2 μm , the mean I/O
406 ratios are in the range of 0.17-0.65 and there is a tendency for the I/O ratio to increase with
407 increasing particle size. For particles of 0.1-1.0 μm , the size-resolved mean I/O ratios are in
408 the range 0.12-0.65. The highest mean I/O ratios occur for particle diameters of
409 approximately 0.3 μm . The mean I/O ratios decrease sharply when the particle size is larger
410 than 0.3 μm . The trend for size-resolved I/O ratios of particles with diameters 0.3-5.0 μm
411 generally agrees with the findings reported by Gupta and Cheong. [32] for ACMV-dominated
412 indoor environments. These findings also align with theoretically predicted results that
413 fibrous particle filters usually have minimum efficiencies for diameters in the range 0.05-0.5
414 μm [11].

415 Figure 5 suggests that, in addition to mechanical ventilation and active filtration, the
416 operation of air conditioning influenced the indoor/outdoor particle ratio. There is a trend
417 such that when the air conditioning was on, the I/O ratios for particles between 0.17 μm and
418 2.5 μm were lower than when the air conditioning was off. Conversely, for particles smaller

419 than about 0.1 μm , there is a tendency for the I/O ratio to be higher when the air conditioning
420 was on as compared to the air-conditioning off state.

421 We have compared the I/O ratios in these two modes using one-way ANOVA tests. The
422 statistical analysis reveals that the differences are statistically significant ($p \leq 0.05$) for
423 particles in all size bins between 0.17 μm and 2.5 μm , except for the size bin 0.3-0.374 μm (p
424 = 0.29). These findings suggest that the ACMV system has higher removal efficiency for
425 particles in this larger size range with active cooling by the air conditioning system.

426 In Singapore's tropical climate, whenever air conditioning is operating, the cooling coil
427 would receive a flow of condensing water from the humid air stream passing over its cooled
428 surfaces. The elevated removal efficiency suggests the possibility of enhanced removal of
429 particles onto the wet surface of the cooling coil when air conditioning is on. The presence of
430 a water film would narrow the gaps between fins. The process of condensation would also
431 induce net transport of particles toward the condensing surfaces through the mechanism of
432 diffusiophoresis. There may also be a thermophoretic influence inducing particle migration
433 from the warmer air toward the cooler fins. It has been recognized that a cooling coil can
434 contribute to removing particles from airstreams [24, 33, 34]. At present, the processes and
435 mechanisms are not well understood and we know of no previously published data of the type
436 presented in Figure 5.

437 For smaller particles, with diameters of 0.01-0.154 μm , we observe a trend of higher I/O
438 ratios when the air conditioning is on compared to when it is off. However, one-way

439 ANOVA results reveal that the differences between the I/O ratios are statistically significant
440 ($p < 0.05$) only for particles in a few size bins, 0.0205–0.0365 μm and 0.0649–0.154 μm .
441 This trend contradicts the theoretically predicted results by Waring and Siegel [34]. In their
442 study, higher deposition rates were predicted for ultrafine particles onto a wet surface than
443 onto the dry surface of a cooling coil. We speculate that the higher I/O ratios that we observe
444 for these smallest particles might be attributable to the growth of ultrafine particles owing to
445 condensation as the air stream is cooled. The condensing species could include water and
446 also semivolatile organic compounds in the air stream whose partitioning between the gas
447 and particle phase is materially influenced by temperature.

448 The information in this study is insufficient to conclusively explain these observations. In
449 future studies, laboratory tests with well-controlled operational parameters could serve to
450 elucidate the influence of cooling coil operation on particle behavior across different size
451 ranges.

452 It is conceivable that variations of outdoor particle concentrations might indirectly influence
453 I/O ratios. However, our data indicate that the difference of time-averaged outdoor particle
454 concentrations between the daytime (AC on) and nighttime (AC off) conditions is relatively
455 small, i.e. less than a 10% difference. Consequently, we consider that variations in outdoor
456 levels did not significantly affect the I/O ratios between the two ACMV operation modes in
457 this investigation.

458 *3.5. Particle removal efficiencies*

459 Figure 6 depicts the time-averaged and size-resolved removal efficiencies of the ACMV
460 system for particles with diameters of 0.01-6.0 μm for two ACMV operation modes (Mode 1:
461 both AC and MV on; Mode 2: AC off and MV on). The single-pass removal efficiencies
462 range from 5% to 80% in both ACMV operation modes, with the respective lowest and
463 highest efficiencies occurring at 0.1 μm and 3.71 μm in Mode 1, and 0.33 μm and 6.0 μm in
464 Mode 2. More specifically, the removal efficiencies are smaller than 30% for particles of
465 diameter 0.01-1.0 μm in Mode 1 and for particles of diameter 0.015-1.12 μm in Mode 2.

466 The size-resolved particle removal efficiencies calculated in the current study have a similar
467 profile with those reported by [Azimi et al. \[35\]](#) (Figure 5 of their paper), which were based on
468 the measured single-pass sized-resolved removal efficiencies for particles of 0.03-10 μm by
469 [Hecker and Hofacre. \[36\]](#).

470 When the mechanical ventilation system was on, indoor air passed through the filters and
471 cooling coil an average of nine times before being replaced by outdoor air, and particle
472 concentrations would diminish during each pass. Consequently, the overall effectiveness of
473 the ACMV system with MERV 7 filters is much higher than the corresponding single-pass
474 efficiency. However, the MERV 7 filters are still insufficient to protect indoor occupants
475 from fine particles of outdoor origin during the haze episode when considering both the low
476 single-pass particle removal efficiencies and the findings reported in Section 3.3. The low
477 removal efficiency of the MERV 7 filters for ultrafine particle also indicates that the filters

478 may fail to protect indoor occupants from ultrafine particles of outdoor origin even during
479 clear-sky periods, when outdoor ultrafine particle number concentrations are elevated
480 (Section 3.2). The high removal efficiencies for particles $> 3 \mu\text{m}$ indicate that the MERV 7
481 filters work effectively to remove the coarse particles. The filters' improved removal
482 efficiencies for coarse particles may be influenced by accumulated particles on the filters as
483 the filters are used.

484 Comparisons of the particle removal efficiencies in the two ACMV operation modes reveal
485 that the removal efficiencies for particles of $0.37\text{-}3.74 \mu\text{m}$ are significantly higher in the AC
486 on mode than in the AC off mode (one-way ANOVA test, $p < 0.05$). The wet cooling coil
487 surface in the AC on mode results in increases of 4-25% in the removal efficiencies for
488 particles with diameters of $0.37\text{-}3.74 \mu\text{m}$ when compared with the dry cooling coil surface in
489 the AC off mode. The findings suggest that during the haze episode, air conditioning
490 operation could contribute to the attenuation of outdoor particles in this size range in indoor
491 air. However, it is also possible that enhanced particle deposition to wet cooling coil surfaces
492 could contribute to fouling of those surfaces over the long term.

493 **4. Conclusions**

494 During the 2013 haze in Singapore, the outdoor mean size distribution of particles larger than
495 $0.2 \mu\text{m}$ in diameter was remarkably higher than on clear days. Overall, particles of $0.1\text{-}1.0$
496 μm accounted for large increases, with aggregate volume concentrations that were 5 to 60
497 times higher than during the clear-sky conditions that prevailed a few weeks after the haze

498 episode. There was an evident size shift of the peak particle size to larger diameters within
499 the accumulation mode. This phenomenon might be a consequence of secondary growth of
500 organic aerosol induced by photochemical reactions during the haze.

501 In a mechanically ventilated and air conditioned room on the NTU campus, equipped with
502 MERV 7 grade filters, indoor particles in the size range 0.3-1.0 μm followed the time pattern
503 of outdoor particle concentrations, with some attenuation and a short lag time. The
504 correlations between indoor and outdoor particles in the size range 1.0-2.5 μm were moderate
505 and correlations were not observed for larger particles. Relative to the clear-sky conditions,
506 indoor concentrations of particles in the size range 0.3-2.5 μm increased by factors of 2 to 14
507 during the haze. Any such increase for larger particles was marginal.

508 The mean I/O ratio and removal efficiency of the ACMV system of particles was observed to
509 vary with particle size as would be expected. A conventional ACMV system with MERV 7
510 filters is insufficient to protect building occupants from high exposures to fine particles of
511 outdoor origin under extraordinary circumstances such as the 2013 haze. More effective
512 strategies to protect the public are needed for the recurring transboundary haze.

513 We observed that both I/O ratios and particle removal efficiencies of the ACMV system
514 varied systematically depending on whether or not the air conditioning was on. Information
515 in the current study is insufficient to fully explain these observations. As yet, there is limited
516 scientific knowledge about how pollutants, such particles, semivolatile organic compounds,

517 bioaerosols, and ozone, interact with cooling coil surfaces. More studies that advance our
518 knowledge of these topics are necessary.

519 **Acknowledgements**

520 The authors thank the Republic of Singapore's National Research Foundation for financial
521 support through grant NRF-CRP8-2011-03 and through a grant to the Berkeley Education
522 Alliance for Research in Singapore (BEARS) for the Singapore-Berkeley Building Efficiency
523 and Sustainability in the Tropics (SinBerBEST) Program. BEARS has been established by
524 the University of California, Berkeley as a center for intellectual excellence in research and
525 education in Singapore.

526 **References**

- 527 [1] Amiridis V, Zerefos C, Kazadzis S, Gerasopoulos E, Eleftheratos K, Vrekoussis M, et al.
528 Impact of the 2009 Attica wild fires on the air quality in urban Athens. *Atmos Environ*
529 2012;46:536-44.
- 530 [2] Popovicheva O, Kistler M, Kireeva E, Persiantseva N, Timofeev M, Kopeikin V, et al.
531 Physicochemical characterization of smoke aerosol during large-scale wildfires: Extreme
532 event of August 2010 in Moscow. *Atmos Environ* 2014;96:405-14.
- 533 [3] Mühle J, Lueker TJ, Su Y, Miller BR, Prather KA, Weiss RF. Trace gas and particulate
534 emissions from the 2003 southern California wildfires. *J Geophys Res* 2007;112:D03307.
- 535 [4] Vicente A, Alves C, Calvo AI, Fernandes AP, Nunes T, Monteiro C, et al. Emission
536 factors and detailed chemical composition of smoke particles from the 2010 wildfire
537 season. *Atmos Environ* 2013;71:295-303.
- 538 [5] Makkonen U, Hellén H, Anttila P, Ferm M. Size distribution and chemical composition of
539 airborne particles in south-eastern Finland during different seasons and wildfire episodes
540 in 2006. *Sci Total Environ* 2010;408:644-51.
- 541 [6] Phoothiwut S, Junyapoon S. Size distribution of atmospheric particulates and particulate-
542 bound polycyclic aromatic hydrocarbons and characteristics of PAHs during haze period
543 in Lampang Province, Northern Thailand. *Air Qual Atmos Health* 2013;6:397-405.
- 544 [7] Franzi LM, Bratt JM, Williams KM, Last JA. Why is particulate matter produced by
545 wildfires toxic to lung macrophages? *Toxicol Appl Pharm* 2011;257:182-8.
- 546 [8] Huttunen K, Siponen T, Salonen I, Yli-Tuomi T, Aurela M, Dufva H, et al. Low-level
547 exposure to ambient particulate matter is associated with systemic inflammation in
548 ischemic heart disease patients. *Environ Res* 2012;116:44-51.

- 549 [9] Wegesser TC, Franzi LM, Mitloehner FM, Eiguren-Fernandez A, Last JA. Lung
550 antioxidant and cytokine responses to coarse and fine particulate matter from the great
551 California wildfires of 2008. *Inhal Toxicol* 2010;22:561-70.
- 552 [10] Viswanathan S, Eria L, Diunugala N, Johnson J, McClean C. An analysis of effects of
553 San Diego wildfire on ambient air quality. *J Air Waste Manag Assoc* 2006;56:56-67.
- 554 [11] Hinds WC. *Aerosol technology: Properties, behavior, and measurement of airborne*
555 *particles, 2nd edition: John Wiley & Sons, New York.; 1999.*
- 556 [12] Radke LF, Hegg AS, Hobbs PV, Penner JE. Effects of aging on the smoke from a large
557 forest fire. *Atmos Res* 1995;38:315-32.
- 558 [13] Niemi JV, Tervahattu H, Vehkamäki H, Martikainen J, Laakso L, Kulmala M, et al.
559 Characterization of aerosol particle episodes in Finland caused by wildfires in Eastern
560 Europe. *Atmos Chem Phys* 2005;5:2299-310.
- 561 [14] Klepeis NE, Nelson WC, Ott WR, Robinson JP, Tsang AM, Switzer P, et al. The
562 National Human Activity Pattern Survey (NHAPS): A resource for assessing exposure to
563 environmental pollutants. *J Expo Anal Env Epid* 2001;11:231-52.
- 564 [15] Thornburg J, Ensor DS, Rodes CE, Lawless PA, Sparks LE, Mosley RB. Penetration of
565 particles into buildings and associated physical factors. Part I: Model development and
566 computer simulations. *Aerosol Sci Tech* 2001;34:284-96.
- 567 [16] Hussein T, Hämeri K, Aalto P, Asmi A, Kakko L, Kulmala M. Particle size
568 characterization and the indoor-to-outdoor relationship of atmospheric aerosols in
569 Helsinki. *Scand J Work Environ Health* 2004;30 (Suppl 2):54-62.
- 570 [17] Koponen IK, Asmi A, Keronen P, Puhto K, Kulmala M. Indoor air measurement
571 campaign in Helsinki, Finland 1999 – the effect of outdoor air pollution on indoor air.
572 *Atmos Environ* 2001;35:1465-77.
- 573 [18] Matson U. Indoor and outdoor concentrations of ultrafine particles in some Scandinavian
574 rural and urban areas. *Sci Total Environ* 2005;343:169-76.
- 575 [19] Wang Y, Hopke PK, Chalupa DC, Utell MJ. Long-term characterization of indoor and
576 outdoor ultrafine particles at a commercial building. *Environ Sci Technol* 2010;44:5775-
577 80.
- 578 [20] Morawska L, Jamriska M, Guo H, Jayaratne ER, Cao M, Summerville S. Variation in
579 indoor particle number and PM_{2.5} concentrations in a radio station surrounded by busy
580 roads before and after an upgrade of the HVAC system. *Build Environ* 2009;44:76-84.
- 581 [21] Shi B, Ekberg LE, Langer S. Intermediate air filters for general ventilation applications:
582 An experimental evaluation of various filtration efficiency expressions. *Aerosol Sci Tech*
583 2013;47:488-98.
- 584 [22] Zhou J, Chen A, Cao Q, Yang B, Chang VWC, Nazaroff WW. Particle exposure during
585 the 2013 Haze in Singapore: Importance of the built environment. *Build Environ*
586 2015;93:14-23.
- 587 [23] Azimi P, Stephens B. HVAC filtration for controlling infectious airborne disease
588 transmission in indoor environments: Predicting risk reductions and operational costs.
589 *Build Environ* 2013;70:150-60.

- 590 [24] Siegel JA, Nazaroff WW. Predicting particle deposition on HVAC heat exchangers.
591 Atmos Environ 2003;37:5587-96.
- 592 [25] Wu J, Zhao B. Effect of ventilation duct as a particle filter. Build Environ 2007;42:2523-
593 29.
- 594 [26] Riley WJ, McKone TE, Lai ACK, Nazaroff WW. Indoor particulate matter of outdoor
595 origin: Importance of size-dependent removal mechanisms. Environ Sci Technol
596 2002;36:200-7.
- 597 [27] Betha R, Zhang Z, Balasubramanian R. Influence of trans-boundary biomass burning
598 impacted air masses on submicron particle number concentrations and size distributions.
599 Atmos Environ 2014;92:9-18.
- 600 [28] Mielonen T, Portin H, Komppula M, Leskinen A, Tamminen J, Ialongo I, et al. Biomass
601 burning aerosols observed in Eastern Finland during the Russian wildfires in summer 2010
602 – Part 2: Remote sensing. Atmos Environ 2012;47:279-87.
- 603 [29] Kulmala M, Vehkamäki H, Petäjä T, Dal Maso M, Lauri A, Kerminen VM, et al.
604 Formation and growth rates of ultrafine atmospheric particles: A review of observations. J
605 Aerosol Sci 2004;35:143-76.
- 606 [30] Betha R, Spracklen DV, Balasubramanian R. Observations of new aerosol particle
607 formation in a tropical urban atmosphere. Atmos Environ 2013;71:340-51.
- 608 [31] Nazaroff WW. Indoor particle dynamics. Indoor Air 2004;14 (Suppl 7):175-83.
- 609 [32] Gupta A, Cheong KWD. Physical characterization of particulate matter and ambient
610 meteorological parameters at different indoor–outdoor locations in Singapore. Build
611 Environ 2007;42:237-45.
- 612 [33] Jamriska M, Morawska L, Clark BA. Effect of ventilation and filtration on
613 submicrometer particles in an indoor environment. Indoor Air 2000;10:19-26.
- 614 [34] Waring MS, Siegel JA. Particle loading rates for HVAC filters, heat exchangers, and
615 ducts. Indoor Air 2008;18:209-24.
- 616 [35] Azimi P, Zhao D, Stephens B. Estimates of HVAC filtration efficiency for fine and
617 ultrafine particles of outdoor origin. Atmos Environ 2014;98:337-46.
- 618 [36] Hecker R, Hofacre K. Development of performance data for common building air
619 cleaning devices (Final Report No. EPA/600/R-08/013). US Environmental Protection
620 Agency, Office of Research and Development/National Homeland Security Research
621 Center Research Triangle Park, NC 2008.
- 622

Figure Captions

Figure 1. Schematic representation of the air-conditioning and mechanical ventilation system for the office, illustrating the flow rates (Q), fans (F), filter and coil in the system. For air-flow rates, the subscripts F , R and EX denote forced supply (make-up), recirculation and exfiltration, respectively.

Figure 2. Size-resolved time-averaged outdoor particle volume concentrations ($dV/d(\log D_p)$) sorted according to four particle pollution categories. The V value in the legend refers to total average particle volume concentration (0.01-10 μm) in each particle size category.

Figure 3. Size-resolved time-averaged outdoor particle number concentrations ($dN/d(\log D_p)$) sorted according to four particle pollution categories. The N value in the legend refers to total average particle number concentration (0.01-10 μm) in each particle size category.

Figure 4. Time-resolved indoor and outdoor particle volume concentrations (dV) in different particle size ranges and for different degrees of haziness.

Figure 5. Size-resolved particle indoor/outdoor (I/O) ratios in two different air-conditioning operation modes (AC on and AC off). Mechanical ventilation was provided at the same volumetric flow rate in both cases. The error bars refer to standard deviations.

Figure 6. Size-resolved particle removal efficiencies (η_i) of the ACMV system in two different air-conditioning operation modes (AC on and AC off). Mechanical ventilation was provided at the same volumetric flow rates in both cases. The error bars refer to standard deviations.

Table 1. Time, date and haze levels used for time-averaged, size-resolved I/O ratio calculations.

AC mode (MV on)	Time	Date	Haziness
AC on	11:21-15:35	14 June 2013	light
	9:00-18:00	17 June 2013	moderate
	13:56-16:59	20 June 2013	heavy
	13:06-17:00	27 June 2013	light
AC off	11:00-14:00	16 June 2013	moderate
	21:00-24:00	22 June 2013	heavy
	21:00-24:00	27 June 2013	light
	00:00-6:00	28 June 2013	light

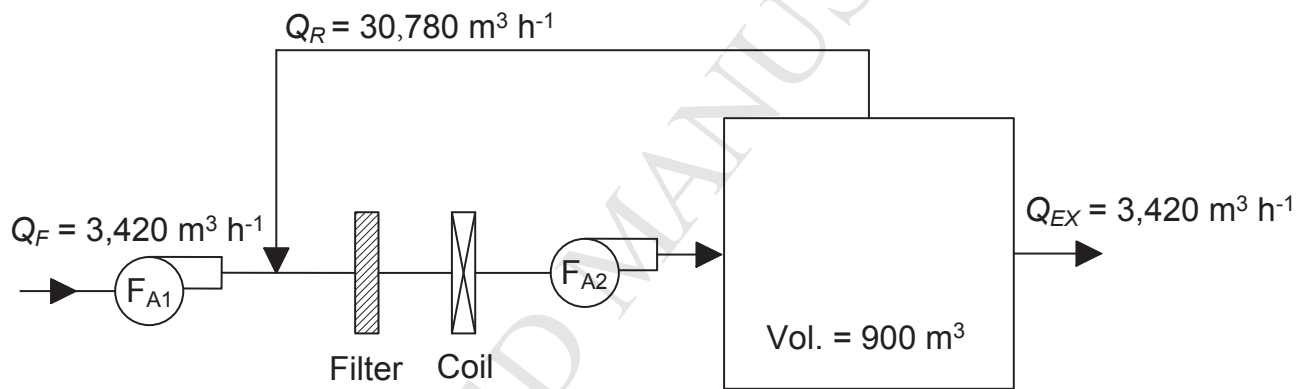


Figure 1. Schematic representation of the air-conditioning and mechanical ventilation system for the office, illustrating the flow rates (Q), fans (F), filter and coil in the system. For air-flow rates, subscripts F , R and EX denote forced supply (make-up), recirculation and exfiltration, respectively.

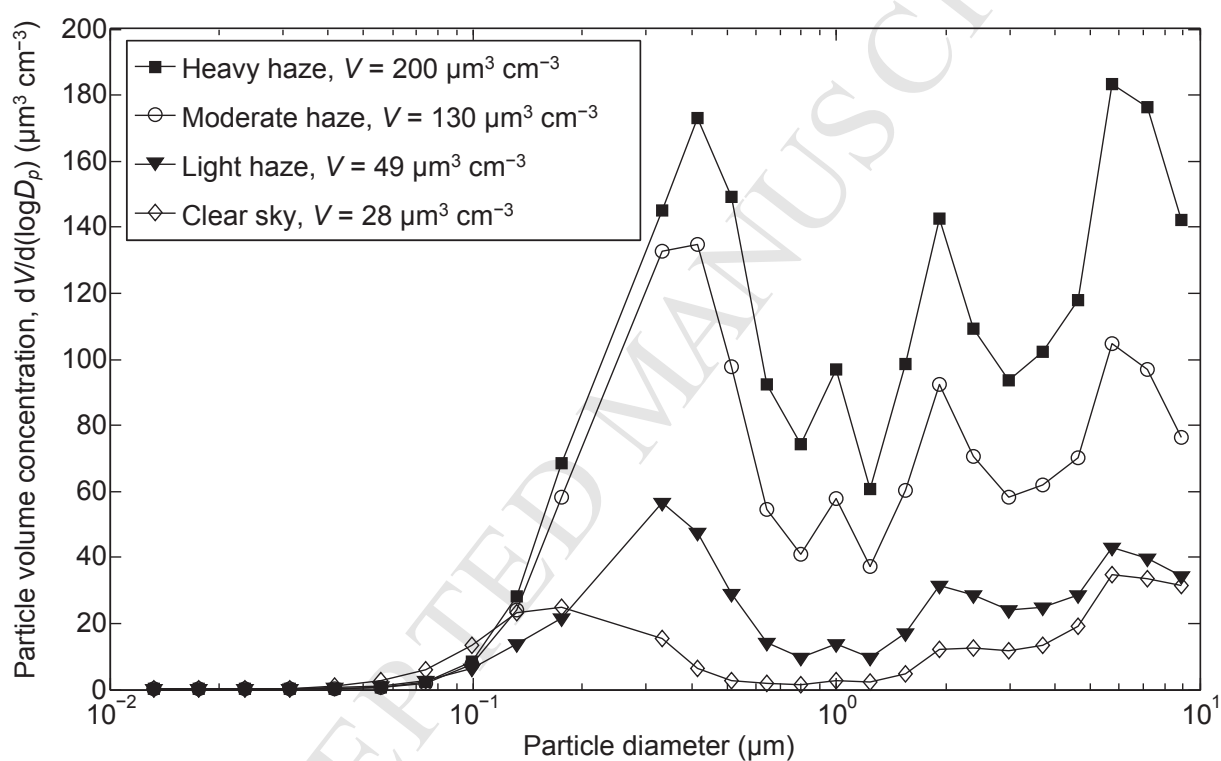


Figure 2. Size-resolved time-averaged outdoor particle volume concentrations ($dV/d(\log D_p)$) sorted according to four particle pollution categories. The V value in the legend refers to total average particle volume concentration ($0.01\text{--}10 \mu\text{m}$) in each particle size category.

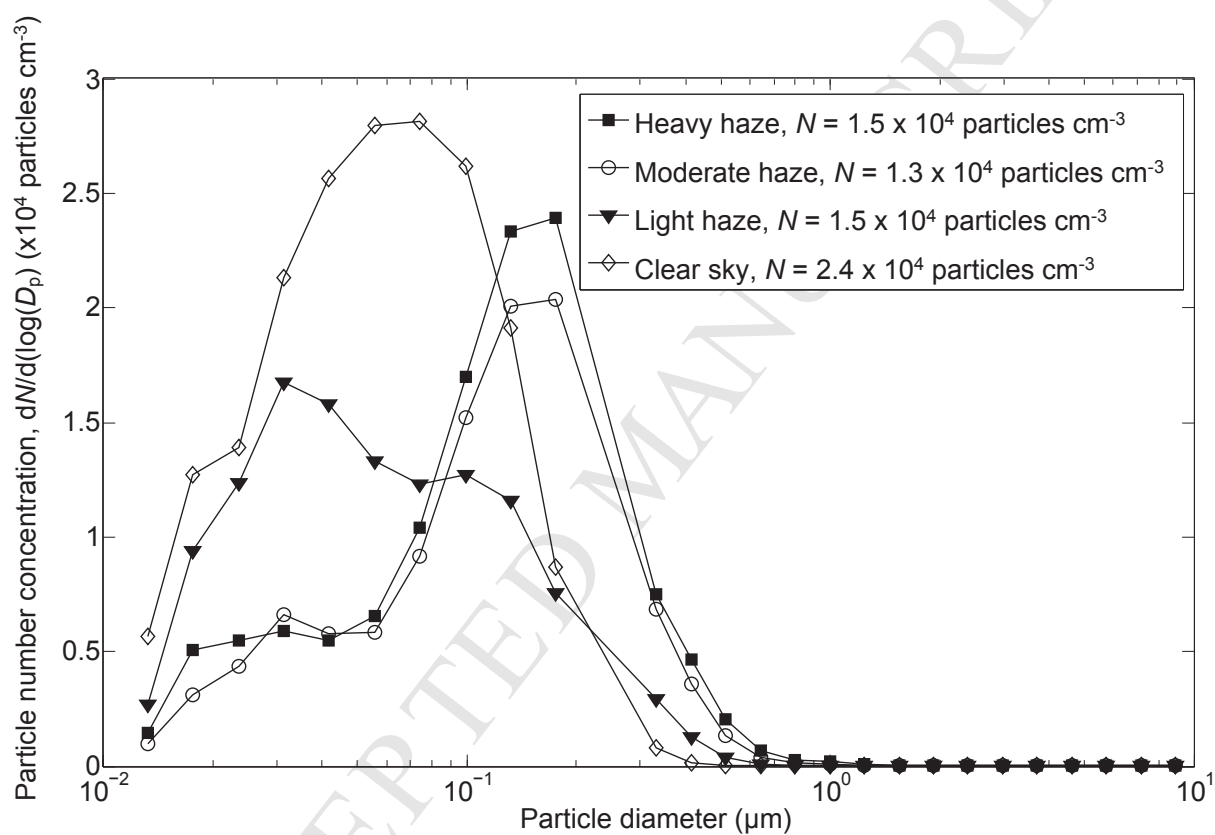


Figure 3. Size-resolved time-averaged outdoor particle number concentrations ($dN/d(\log D_p)$) sorted according to four particle pollution categories. The N value in the legend refers to total average particle number concentration ($0.01\text{--}10 \mu\text{m}$) in each particle size category.

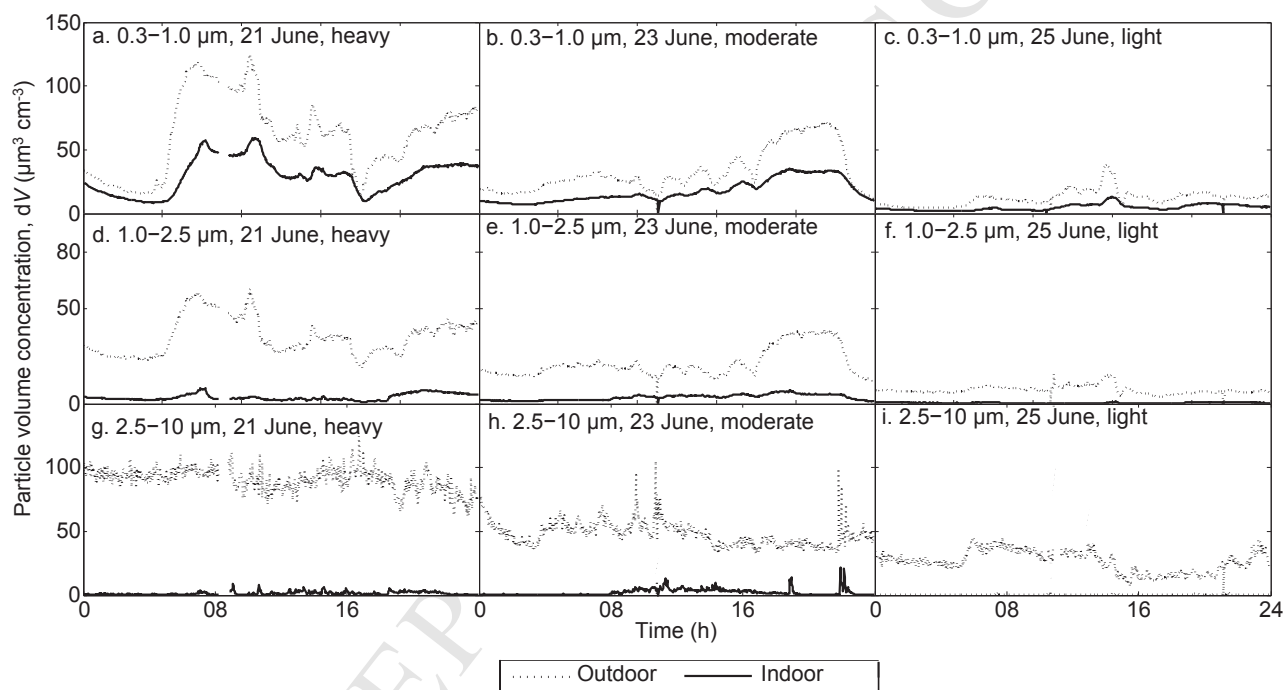


Figure 4. Time-resolved indoor and outdoor particle volume concentrations (dV) in different particle size ranges and for different degree of haziness.

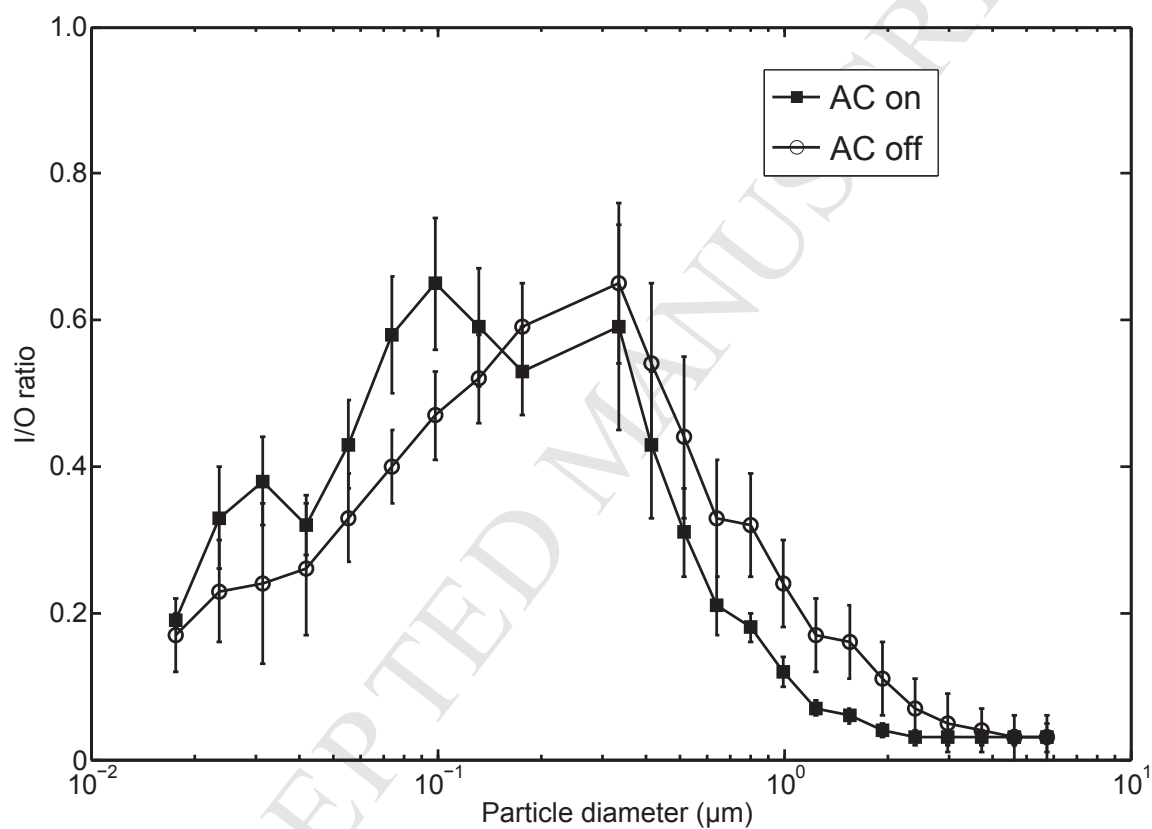


Figure 5. Size-resolved particle indoor/outdoor (I/O) ratios in two different air-conditioning operation modes (AC on and AC off). Mechanical ventilation was provided at the same volumetric flow rates in both cases. The error bars refer to standard deviations.

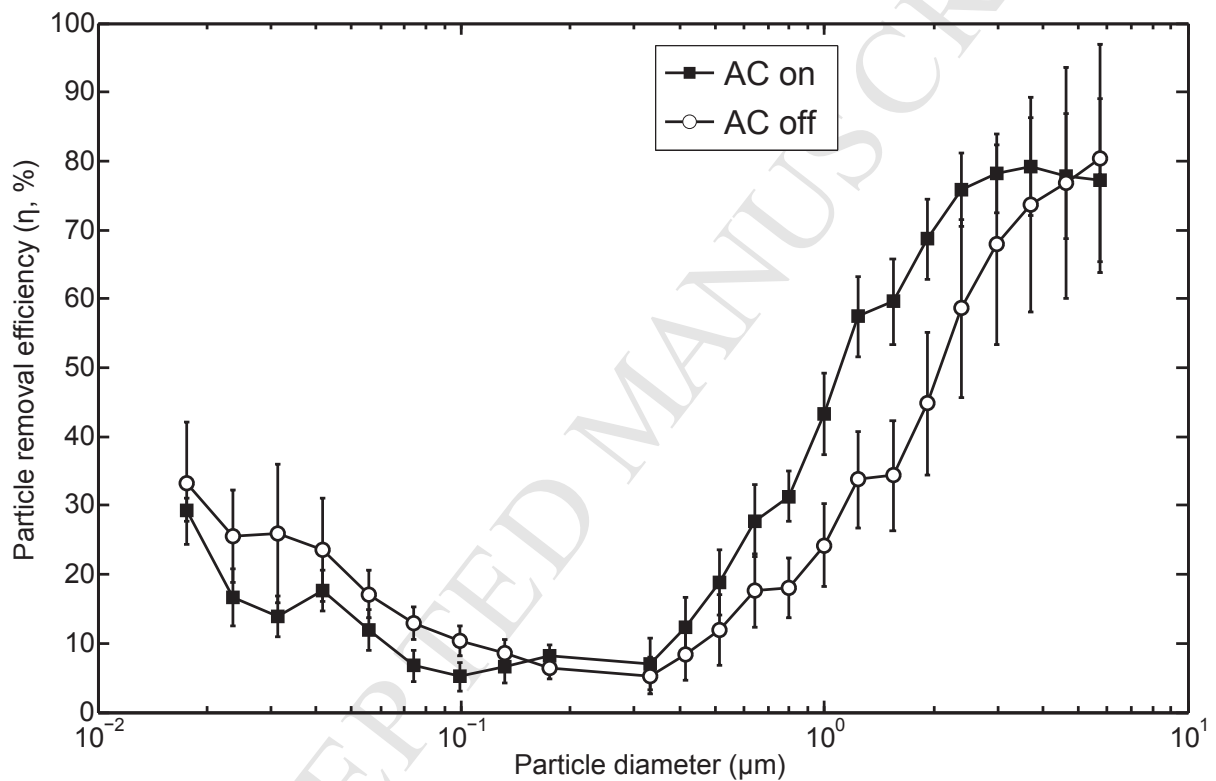


Figure 6. Size-resolved particle removal efficiencies (η_i) of the ACMV system in two different air-conditioning operation modes (AC on and AC off). Mechanical ventilation was provided at the same volumetric flow rates in both cases. The error bars refer to standard deviations.

HIGHLIGHTS (Chen et al., *Building and Environment*, 2015)

- Monitored indoor and outdoor particles during and after the 2013 haze in Singapore.
- Haze mainly causes increases in concentrations of particles larger than $\sim 0.2 \mu\text{m}$.
- ACMV system attenuated penetration and persistence of outdoor particles indoors.
- AC operation altered the indoor/outdoor concentration ratios of fine particles.
- MERV 7 filters provided $< 30\%$ removal efficiencies for particles of $0.01\text{-}1.0 \mu\text{m}$.